Testing of the On-board Attitude Determination and Control Algorithms for SAMPEX

Jon D. McCullough[1], Thomas W. Flatley [1], Debra A. Henretty[2],
F. Landis Markley [3], and Josephine K. San [1]

Algorithms for on-board attitude determination and control of the Solar, Anomalous, and Magnetospheric Particle Explorer (SAMPEX) have been expanded to include a constant gain Kalman filter for the spacecraft angular momentum, pulse width modulation for the reaction wheel command, an algorithm to avoid pointing the Heavy Ion Large Telescope (HILT) instrument boresight along the spacecraft velocity vector, and the addition of digital sun sensor (DSS) failure detection logic. These improved algorithms were tested in a closed-loop environment for three orbit geometries, one with the sun perpendicular to the orbit plane, and two with the sun near the orbit plane - at Autumnal Equinox and at Winter Solstice. The closed-loop simulator was enhanced and used as a truth model for the control systems' performance evaluation and sensor/actuator contingency analysis. The simulations were performed on a VAX 8830 using a prototype version of the on-board software.

Introduction

SAMPEX, the first in the Small Explorer (SMEX) series, will be launched by a Scout launch vehicle from the Western Test Range in June 1992. The mission is designed to obtain scientific data on several different natural phenomena. A statistically large sample of anomalous cosmic ray oxygen nuclei will be obtained to estimate their ionization state. The intensity, latitude, and local time dependence of the precipitating magnetospheric particle fluxes, particularly relativistic electrons, will be continuously recorded. In addition, the SAMPEX mission hopes to detect solar flare events from a low altitude, near-polar orbit during the declining phase of solar activity. The scientific instruments on board are the Low Energy Ion Composition Analyzer (LEICA), the Heavy Ion Large Telescope (HILT), the Mass Spectrometer Telescope (MAST), and the Proton/Electron Telescope (PET).

The spacecraft mechanical configuration is shown in Fig. 1. The SAMPEX spacecraft has a body-fixed pair of solar arrays pointed in the "+y" direction and an experiment complement looking along the "+z" axis. The yaw axis is oriented along the instrument boresights, the pitch axis perpendicular to the solar panels, and the roll axis completes the orthonormal triad. The locations of some of the Attitude Control System (ACS) hardware and science instruments are shown in Fig. 2. The ACS hardware consists of one momentum wheel, three torquer bars, one two-axis fine sun sensor, five coarse sun sensors, and one three-axis magnetometer. The nominal attitude control system function is to point the solar arrays continuously within 5 degrees of the sun and to rotate the spacecraft around the sun line at a rate of 1 revolution per orbit, keeping the experiment axis pointed generally away from the earth. For a complete discussion of the ACS control laws, see Forden, et. al. (Ref. 1). The ACS control laws can be briefly summarized as follows:

---

[1] *Aerospace Engineer, Guidance and Control Branch, NASA/GSFC.*
[2] *Aerospace Engineer, Guidance and Control Branch, NASA/GSFC; Member AIAA.*
[3] *Assistant Branch Head, Guidance and Control Branch, NASA/GSFC; Associate Fellow AIAA, Senior Member AAS.*

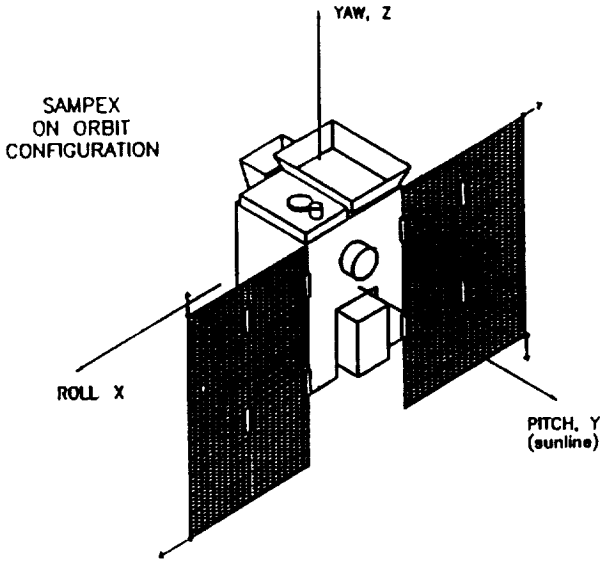

Fig. 1

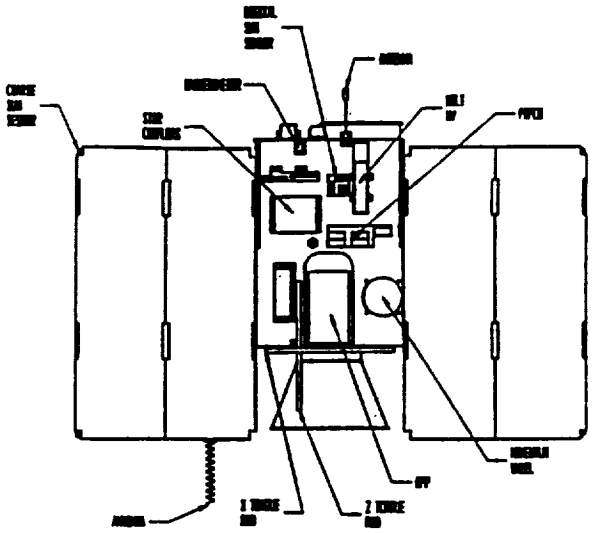

Fig. 2

Initial Acquisition

The spacecraft is inserted into orbit by a spin-stabilized solid rocket motor. Following separation from the launch vehicle and a yo-yo despin, sun pointing must be achieved from an essentially unknown attitude and rate initial state. A small momentum wheel along the intended sun-pointing axis (+y) is spun up to a constant speed, and a conventional three-axis "B-dot" analog controller is used to damp residual body rates. This controller uses a three-axis magnetometer as a sensor and three magnetic torquer bars as actuators.

The despun spacecraft then has a momentum bias along the y-axis (due to the momentum wheel) and the sun sensors are used to determine a sun-pointing error. There are coarse sun sensors which essentially measure the direction cosines of the sun vector in body coordinates for all attitudes and a single two-axis digital sun sensor whose boresight is aligned with the +y axis. The digital sun sensor output is used for control whenever it indicates "sun presence".

Using sun sensor and magnetometer data, precession control logic drives the y-axis torquer bar in a bang-bang fashion to generate torques which precess the momentum vector toward the sun. During this maneuver, the "B-dot" controller acts as a nutation damper.

Normal Control

No additional equipment is employed for so-called "normal" control. Because of the modest pointing accuracy required, the spacecraft is controlled using on-board attitude determination based on the "Algebraic Method" (Ref. 2), probably for the first time ever. This method is based on the fact that if two vectors are known in both body coordinates and in inertial space, the attitude (as represented by an inertial-to-body transformation matrix A) can be unambiguously determined by simple matrix manipulations.

When the spacecraft is in sunlight, the two vectors here are the sun vector and the magnetic field vector. The sensors mentioned determine the components of these vectors in body

coordinates, but their inertial counterparts must be computed on-board based on uplinked ephemeris information and a spherical harmonic magnetic field model. When the spacecraft is in the shadow of the earth, the system angular momentum vector, which is assumed to be inertially fixed due to the pitch axis momentum bias, is used along with the magnetic field vector for attitude determination.

Once A is determined, its derivative is approximated and classical matrix manipulations produce estimated three-axis body rates. Those rates, and the momentum wheel speed are then used to calculate an angular momentum vector. We would like this momentum vector ($\mathbf{H}$) to have some amplitude, say H_0 , and be aligned with the sun, i.e. $\mathbf{H} = H_0\mathbf{S}$. For no nutation we would also like to have it aligned with the +y axis, $\mathbf{H} = H_0\mathbf{j}$. We define a momentum error $\Delta\mathbf{H}$ by

$$\Delta\mathbf{H} = (\mathbf{H} - H_0\mathbf{S}) + (\mathbf{H} - H_0\mathbf{j}) = 2\mathbf{H} - H_0(\mathbf{S} + \mathbf{j})$$

and use the familiar $\mathbf{H} \times \mathbf{B}$ magnetic unloading law to drive the torquer bars for control, i.e. the commanded dipole moment $\mathbf{M}$ is given by

$$\mathbf{M} = k\Delta\mathbf{H} \times \mathbf{B},$$

where k is a gain factor.

The momentum wheel, in addition to providing a momentum bias, is used in a "pitch control loop" to achieve the desired 1 rpo spin rate and "away from the earth" experiment pointing. The yaw axis (the boresights of the instruments) points as close to north as possible at the northernmost point of the orbit, as close to south as possible at the southernmost point of the orbit, and close to the equator at the equatorial crossings. The north pole vector $\mathbf{NP}$ and orbit normal vector $\mathbf{N}$ in GCI coordinates are given as:

$$\mathbf{NP} = [0\ 0\ 1]^T \qquad \text{and} \quad \mathbf{N} = \mathbf{R} \times \mathbf{V} / |\mathbf{R} \times \mathbf{V}|,$$

where $\mathbf{R}$, $\mathbf{V}$ are the inertial position vector and inertial velocity vector of the spacecraft, respectively, estimated from the uplinked ephemeris data. The orbit angle as measured from the northernmost point in the orbit is computed from the two vectors:

$$\mathbf{AN} = \mathbf{NP} \times \mathbf{N} / |\mathbf{NP} \times \mathbf{N}|,$$

the unit vector in the direction of the ascending node, and

$$\mathbf{NMP} = \mathbf{N} \times \mathbf{AN},$$

the unit vector in the direction of the northernmost point of the orbit. The sine and cosine of the orbit angle can now be computed,

$$\sin\alpha = -\mathbf{R}\bullet\mathbf{AN} / |\mathbf{R}|, \qquad \cos\alpha = \mathbf{R}\bullet\mathbf{NMP} / |\mathbf{R}|.$$

The target vector $\mathbf{U}$ must lie in the plane perpendicular to the sun. The following two vectors provide an orthonormal basis for the target vector $\mathbf{U}$:

$$\mathbf{W} = \mathbf{NMP} \times \mathbf{S} / |\mathbf{NMP} \times \mathbf{S}|, \qquad \mathbf{S} \times \mathbf{W}.$$

$\mathbf{W}$ is a unit vector perpendicular to the sun that lies close to the equatorial plane. Thus when the spacecraft is near the equator, we would like $\mathbf{U}$ to point along $\mathbf{W}$. This corresponds to orbit angles of $\alpha = \pi / 2$ and $\alpha = 3\pi / 2$. The unit vector $\mathbf{S} \times \mathbf{W}$ is also perpendicular to the sun and points as close to the northernmost point as possible, given the sun constraint. Thus when the spacecraft is near the poles, we would like $\mathbf{U}$ to point along $\mathbf{S} \times \mathbf{W}$. This corresponds to orbit angles of $\alpha = 0\ ,\ \pi$. Since it is desired to rotate the yaw axis about the positive sun line, the orientation of the orbit normal relative to the sun line must be taken into consideration. A candidate for the target vector $\mathbf{U}$ is

$$\mathbf{U}_{\text{orr}} = \cos\alpha(\mathbf{S} \times \mathbf{W}) + \text{TargetSign}\ \sin\alpha\mathbf{W},$$

where TargetSign is set equal to the negative of SIGN(**S**·**N**) whenever the spacecraft comes within 0.5 degrees of the northernmost or southernmost point of the orbit. This avoids a 180 degree pitch flip if the sun passes through the orbit plane when the spacecraft is near the equator.

For the case where the sun is perpendicular to the orbit plane, the orbit rate rotation mode reduces to a zenith pointing mode. Fig. 3 shows that

$$\mathbf{S} = \mathbf{N}, \qquad \mathbf{W} = \mathbf{NMP} \times \mathbf{S}, \qquad \mathbf{NMP} = \mathbf{S} \times \mathbf{W},$$

and the orientation of the yaw axis along the orbital path is zenith pointing.

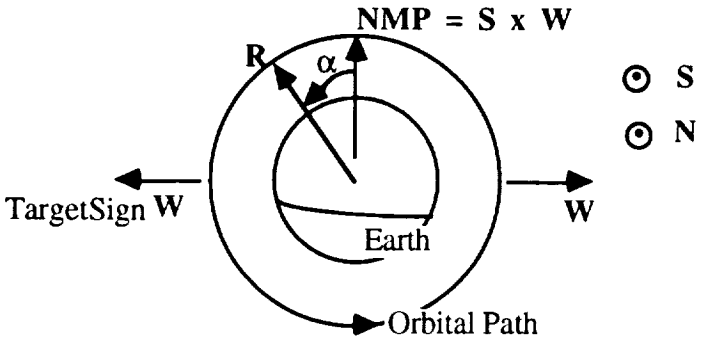

Fig. 3a ORR Mode Geometry When Sun Is Perpendicular To Orbit Plane

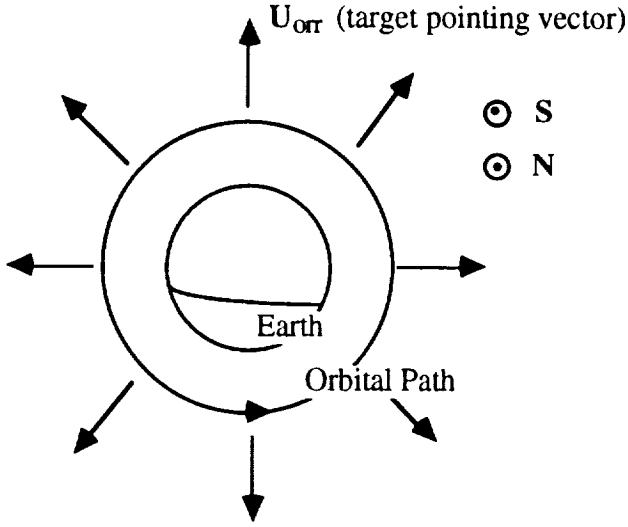

Fig. 3b ORR Mode Target Pointing Vector Along The Orbital Path With Sun Perpendicular To Orbit Plane

For the case where the sun is parallel to the orbit plane, the orbit rate rotation mode becomes a zenith pointing mode over the poles and points in the $\mathbf{R} \times \mathbf{NMP}$ direction at the equator. Fig. 4a shows that $\mathbf{W} = \mathbf{NMP} \times \mathbf{S}$, and so the orientation of the yaw axis can be determined throughout the orbital path and is shown in Fig. 4b.

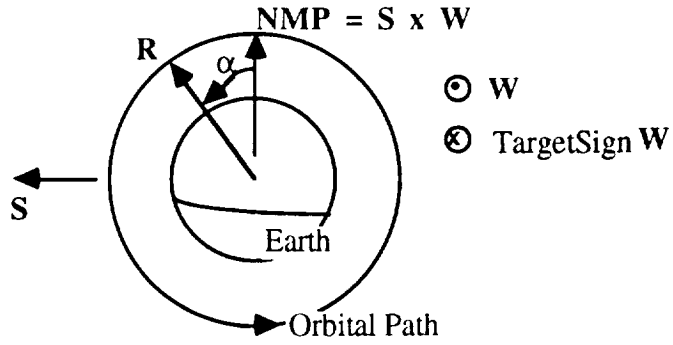

Fig. 4a ORR Mode Geometry When Sun Is In Orbit Plane

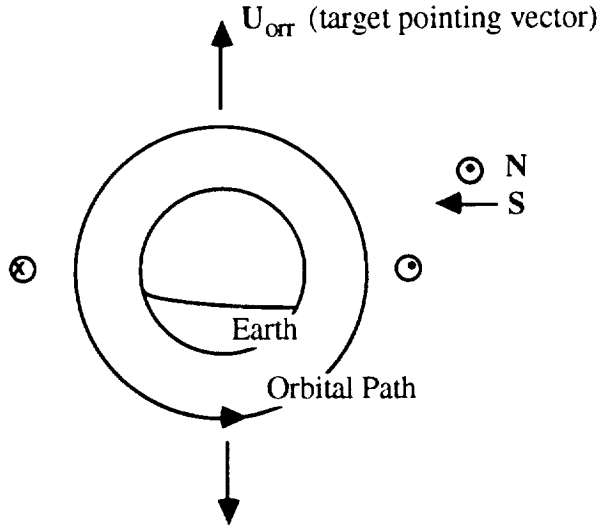

Fig. 4b ORR Mode Target Pointing Vector Along The Orbital Path With Sun Parallel To Orbit Plane

System Angular Momentum Filter

The attitude matrix $A(t)$ is computed at $\Delta t = 0.5$ second intervals, and the least significant bit of the DSS output is 0.5 degrees. Therefore, if the angular velocity is computed by simply back-differencing the attitude matrix, as described above, the roll and yaw rates in sunlit portions of the orbit (the components depending on the DSS data) will be computed as either zero or one degree per second. These exceedingly noisy inputs to the control algorithm produced poor pointing performance in simulations, so it was decided to filter the rate estimates. Let the "derived" system angular momentum in the spacecraft body frame be given by

$$\mathbf{H}_{\text{derived}} = I\omega + H_{\text{wheel}}\mathbf{j},$$

where I is the spacecraft moment-of-inertia tensor, ω is the (noisy) angular velocity vector derived from the attitude matrix, H_{wheel} is the wheel angular momentum (computed from its moment of inertia and tachometer data), and $\mathbf{j}$ is the wheel axis (pitch) unit vector. We

can also predict the system angular momentum at time t based on its dynamics by

$$\mathbf{H}_{\text{predicted}}(t) = A(t)A^{\mathrm{T}}(t - \Delta t)\mathbf{H}(t - \Delta t) + (\mathbf{M} \times \mathbf{B})\Delta t,$$

where $\mathbf{M} \times \mathbf{B}$ is the magnetic control torque in body coordinates. Other external torques are ignored, a reasonable approximation. The reaction wheel torque does not affect the total system angular momentum, of course; it merely shifts the momentum between the spacecraft body and the wheel. The filtered angular momentum is computed as the linear combination

$$\mathbf{H} = (1 - K)\mathbf{H}_{\text{predicted}} + K\mathbf{H}_{\text{derived}},$$

where K is a gain constant. This is referred to as a "constant-gain Kalman filter," although it is too simple to justify this name. The default value of K is 0.01, which corresponds to a time constant of 100 control cycles, or 50 seconds. Simulations show that this gives much smoother performance without introducing excessive lag into the control.

Velocity Avoidance Algorithm

Within 2000 kilometers of the earth's surface, there are 3,000,000 kilograms of orbital debris (Ref. 3), consisting of fragments from explosions, solid rocket effluent, paint flecks, waste, refuse, etc. There are 6,645 orbiting objects currently being tracked which comprise 99.9% of the total mass of all orbiting objects. However, untrackable orbiting pieces (diameter less than 10 cm) number in the millions and are potentially catastrophic or at the least mission degrading (Ref 4). These pieces are almost all in high inclination circular orbits with velocities on the order of 10 km/sec. The EnviroNET (Ref. 5) orbital debris model was used to calculate fluxes for the SAMPEX mission. The assumptions and equations used in computing the fluxes can be found in Kessler, et. al. (Ref. 3).

The HILT proportional counter has a triple entrance foil system with 80μm combined thickness. However, it has the effectiveness of a 380μm single foil for a particle velocity and density of 15 km/sec and 1 gm/cm^3, respectively. Using these results and triple foil penetration limit equations, the smallest particle of concern for the HILT sensor has been determined by Klecker (Ref. 6) to be 0.01 cm.

Meteoroids are part of the interplanetary environment and have average velocities of 20 km/sec with respect to the earth's orbital space. There are 200 kg of meteoroid mass within 2000 km of the earth's surface and most of the mass is concentrated in particles of diameter 0.01 cm (Ref. 3). This coincides with the smallest particle of concern for the HILT sensor. The EnviroNET meteoroid model was used to calculate fluxes for the SAMPEX mission, using assumptions and equations found in Grun, et. al. (Ref. 7); and it was found that orbital debris is significantly more hazardous than micrometeoroids for the SAMPEX mission (Ref. 8). The maximum flux was found to be in the direction of the velocity vector and to be reduced by a factor of 3 for an 80 degree ram angle.

The velocity avoidance algorithm to protect the HILT sensor from hazardous debris is discussed in Reference 8. The velocity avoidance feature, if desired, can be turned on and off by a ground command. Let

$\mathbf{V}$	- unit velocity vector (body coordinates)
$\mathbf{U}$	- target vector
$\varphi_{\min}$	- minimum ram angle (currently 90 degrees)

If $\mathbf{V} \cdot \mathbf{U} \leq \cos\varphi_{\min}$, then the velocity avoidance algorithm is unnecessary. The spacecraft target vector is determine by the orbit rate rotation mode. However, if $\mathbf{V} \cdot \mathbf{U} > \cos\varphi_{\min}$, then the algorithm is implemented.

The algorithm is defined in the Flatley coordinate system. Let the sun unit vector **S** be the 1 axis, the normal science mode target vector **U** be the 3 axis (which by construction is already perpendicular to the sun vector), and $\mathbf{U} \times \mathbf{S}$ be the 2 axis, as defined in Fig. 5.

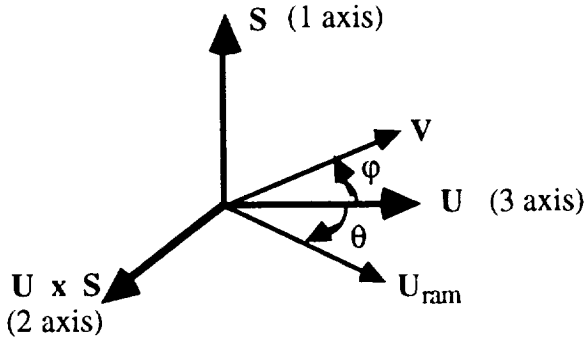

Fig. 5 Flatley Coordinate System

The unit velocity vector **V** and the target vector with velocity avoidance $\mathbf{U}_{ram}$ can be expressed in the Flatley coordinate system as

$$\mathbf{V}_F = [\ V_{F1} \quad V_{F2} \quad V_{F3}\ ]^T, \qquad \mathbf{U}_{ram} = [\ 0 \quad \sin\theta \quad \cos\theta\ ]^T.$$

The desired constraint, $\mathbf{U}_{ram} \cdot \mathbf{V}_F = \cos\varphi_{min}$, is used to determine $\mathbf{U}_{ram}$. This implies

$$V_{F3}\cos\theta = \cos\phi_{min} - V_{F2}\sin\theta.$$

Squaring both sides and using a trigonometric identity results in a quadratic equation for $\sin\theta$ with the solution

$$\sin\theta = \frac{V_{F2}\cos\varphi_{min} \pm |V_{F3}|\sqrt{V_{F2}^2 + V_{F3}^2 - \cos^2\varphi_{min}}}{(V_{F2}^2 + V_{F3}^2)}.$$

If $V_{F2} \geq 0$, then $\sin\theta < 0$ and the negative sign is chosen for the radical. If $V_{F2} < 0$, then $\sin\theta > 0$ and the positive sign is chosen for the radical. Thus $\mathbf{U}_{ram}$ is given by

$$\mathbf{U}_{ram} = \sin\theta(\mathbf{U} \times \mathbf{S}) + \cos\theta\ \mathbf{U}.$$

The testing of the velocity avoidance algorithm is descibed in detail in Reference 8, and can be summarized as follows. For the best case orbit geometry (sun in the orbit plane), there is a small sun pointing error (< 0.3°) for all minimum ram angles. Only for the 100° minimum ram angle does the zenith offset, the angle between zenith and the spacecraft yaw axis, become significant, reaching approximately 10 degrees. The velocity avoidance scheme keeps the yaw axis pointed at least the desired minimum ram angle away from the velocity vector, and science pointing performance is not affected by including the velocity avoidance algorithm.The worst case orbit geometry (sun in the orbit plane) dramatically illustrates the effect of increasing the minimum ram angle. The sun pointing error increases from 1° to 2°. The zenith offset and the ram angle show that the spacecraft flips when the minimum ram angle reaches 100°. Also, science pointing performance begins to decrease

significantly for increasing minimum ram angles. Intermediate cases were also considered in Reference 8.

Table 1 shows the percent of the orbit that the spacecraft is pointing within 15 degrees of zenith. These numbers were calculated for the periods of the orbit where the spacecraft was within 60 degrees of either pole. This table demonstrates how well the science pointing requirement is satisfied while maintaining the five degree sun pointing requirement.

Table 1 - SCIENCE POINTING PERFORMANCE (percent of orbit)

	best case	intermediate case	worst case
No Avoidance	100.0	68.9	0.0
80 deg ram	100.0	68.9	4.9
90 deg ram	100.0	59.3	4.7
100 deg ram	100.0	27.0	11.2

The probability of survival for the HILT sensor was computed for the orbit rate rotation mode with and without the velocity avoidance scheme (Ref. 8), with the results shown in Table 2.

Table 2 - HILT SURVIVAL ESTIMATES

Mode	Mean Flux (coll/m^2 yr)	τ (yrs/coll)	P_S (%)
ORR	3.11485	21.690	87.1
ORR w/ 80° ram	2.92332	23.111	87.8
ORR w/ 90° ram	2.68487	25.164	88.8
ORR w/100° ram	1.90232	35.515	91.9

Sun Sensor Failure Detection Logic

The Small Explorer spacecraft, including SAMPEX, are designed as single-string systems with very little ACS sensor and actuator redundancy. The only sensor redundancy on SAMPEX is that the sun vector can be obtained from either the digital sun sensor (DSS) or the coarse sun sensor (CSS) eyes. Since the sun-pointing constraint is critical for powering the spacecraft, it is desirable to substitute CSS data for DSS data in the unlikely event of failure of the latter sensor.

The logic to decide which sun sensor to trust makes use of the fact that the dot product of two vectors is frame-independent, specifically the dot product of the sensed sun vector and magnetic field **B** in the body and the dot product of the modeled sun vector and magnetic field in inertial space. Thus the ACS performs three tests on each control cycle when the spacecraft is in sunlight:

DSS and CSS disagree if $\cos^{-1}(\mathbf{S}_{CSS} \bullet \mathbf{S}_{DSS}) >$ CSS tolerance,

CSS and models disagree if $\left|\cos^{-1}(\mathbf{S}_{CSS} \bullet \mathbf{B}) - \cos^{-1}(\mathbf{S}_{model} \bullet \mathbf{B}_{model})\right| >$ CSS tolerance,

DSS and models disagree if $\left|\cos^{-1}(\mathbf{S}_{DSS} \bullet \mathbf{B}) - \cos^{-1}(\mathbf{S}_{model} \bullet \mathbf{B}_{model})\right| >$ DSS tolerance.

The DSS tolerance is conservatively set to 5°, to allow for a combination of sensor and modeling errors. The CSS tolerance is much larger, 30°, to allow for earth albedo corruption of the CSS sun vector.

If the DSS agrees with either the models or the CSS, the ACS uses the sun vector computed from DSS data. If the DSS disagrees with both the CSS and the models, but the CSS and models agree, the ACS sets a flag indicating that the DSS data are bad and uses the sun vector computed from CSS data. In all other cases of disagreement, it is not possible to determine whether the DSS, the CSS, the magnetometer, or the models (including the onboard ephemeris) are in error, so the data source for computing the sun vector is left unchanged.

If SAMPEX enters safehold, the analog safehold control will use DSS data if available. Thus it is desirable to turn off the DSS by ground command if telemetry shows that the DSS data are consistently bad.

Contingency Analyses

Through the use of the closed-loop simulator, tests were run to ascertain the performance and stability of spacecraft control in the presence of sensor or actuator failures. The simulations were run for a 9 p.m. orbit in which the aerodynamic torques on the spacecraft are greatest. Some of the tests are summarized below.

DSS Failures

The two-axis DSS that will be used on SAMPEX consists of two measurement components mounted at right angles that yield a 128 x 128 degree Field of View (FOV). The two measurement components generate two eight bit Gray-coded outputs which are digital representations of the angle between the sunline and the normal to the sensor when the sun is in the FOV of the command component (Ref. 9). The purpose of the command component is to indicate when there is sun presence. These outputs are then converted to two eight bit binary outputs which are translations of the Gray-coded outputs and have values (counts) ranging from 0 to 255. Simulations were run to evaluate spacecraft controllability for failures in both the Most Significant Bit (MSB) and the second bit of the Gray-coded output.

The MSB, or sign bit, determines which side of the sensor the sun is on, and can fail to either 0 or 1. Since both of these failures result in similar behavior, a true reading on one side of the boresight and a false reading (error signal with the opposite sign) on the other side of the boresight, only one of these failures was modeled. This is illustrated in Fig. 6.

The plot of the Sun Pointing Error (Fig. 7) shows an average error of approximately 15 degrees in ORR mode for a failure in the sign bit. The failure was initiated 3,000 seconds into the run so that it could be modeled in steady-state. The plot of the Bad FSS Flag (Fig. 8) shows continual shifting between the CSS and DSS. As long as the truth models agree with the DSS and the CSS to within 30 degrees, the Bad FSS Flag is not toggled and the spacecraft may be controlled entirely by the failed DSS. This is a result of the way the DSS/CSS switching logic is implemented and can result in the spikes shown in the Sun Pointing Error.

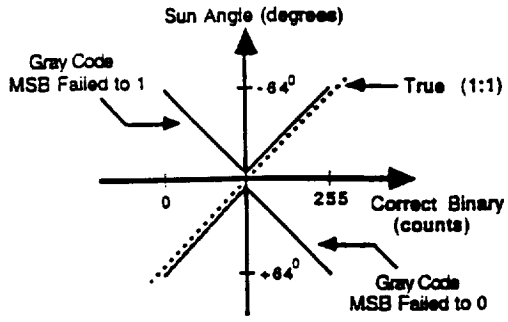

Fig. 6 Sun Angle with a Failure in the MSB

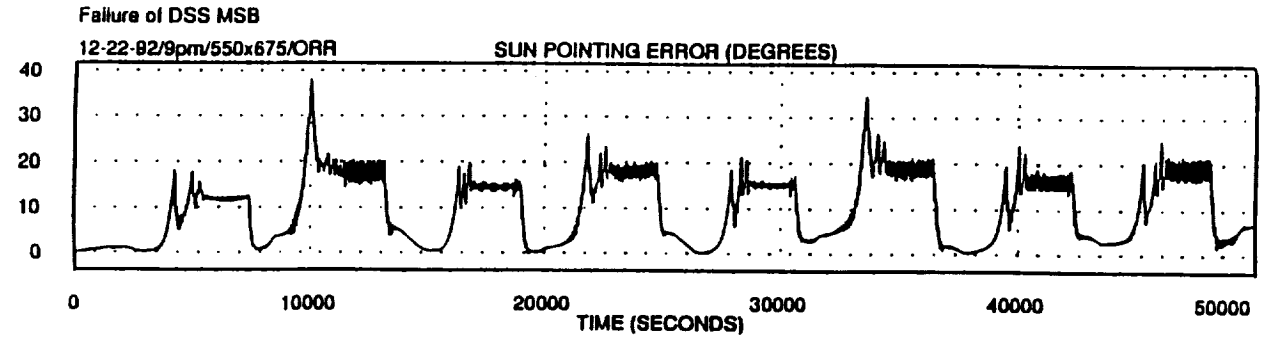

Fig. 7 Sun Pointing Error (Failure of DSS MSB)

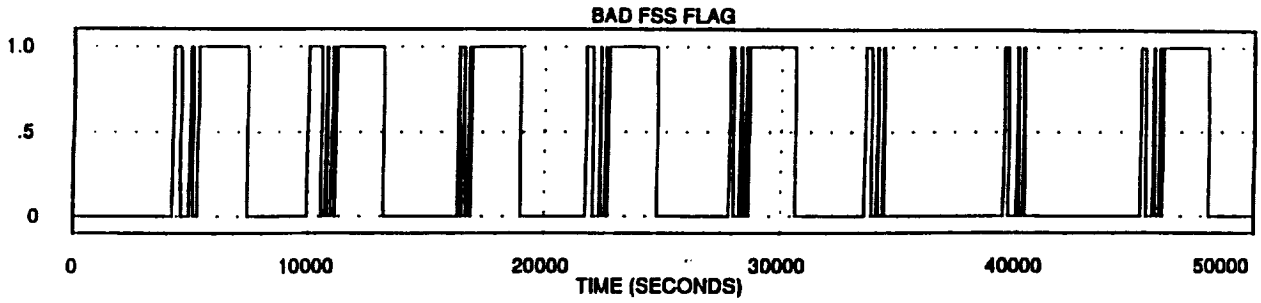

Fig. 8 Bad FSS Flag (Failure of DSS MSB)

The failure of the second bit to either a 0 or 1 results in very different behaviors, as illustrated in Fig. 9. Both of these failures were modeled and are discussed below.

A failure of the 2nd bit to 0 results in a "bang-bang" control since the effective Least Significant Bit (LSB) of the DSS becomes 64 degrees near null rather than 0.5 degrees, causing the pitch axis to move away from the sun. The simulation shows that this failure of the DSS is easily detected and the spacecraft is controlled entirely by the CSS. The plot of the Sun Pointing Error (Fig. 10) for a 2nd bit failure to 0 shows that the average error is

approximately 6 degrees in ORR mode, which reflects the +/- 6 degree blind spot of the CSS on the positive pitch axis.

A failure of the 2nd bit to 1 results in a very benign failure as long as the spacecraft remains within 32 degrees of the sun, since the second bit of the Gray code should be 1 in this case. However, if the spacecraft is pointing between 32 degrees and 64 degrees of the sun there will be an error in the DSS. This computed pointing error will be smaller than the true sun error but will be of the correct sign. The plot of the Sun Pointing Error (Fig. 11) shows that the spacecraft pitch axis remains within 32 degrees of the sun in ORR, and a failure in the 2nd bit is never detected. Thus, the DSS continues to control the spacecraft maintaining a sun pointing error of less than 5 degrees.

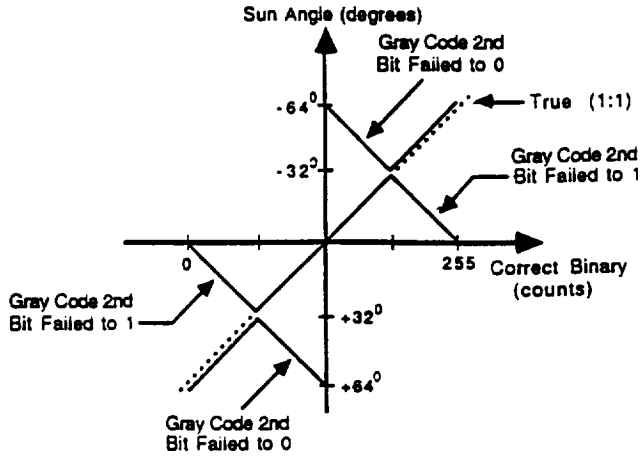

Fig. 9 Sun Angle (DSS Failure of 2nd Bit)

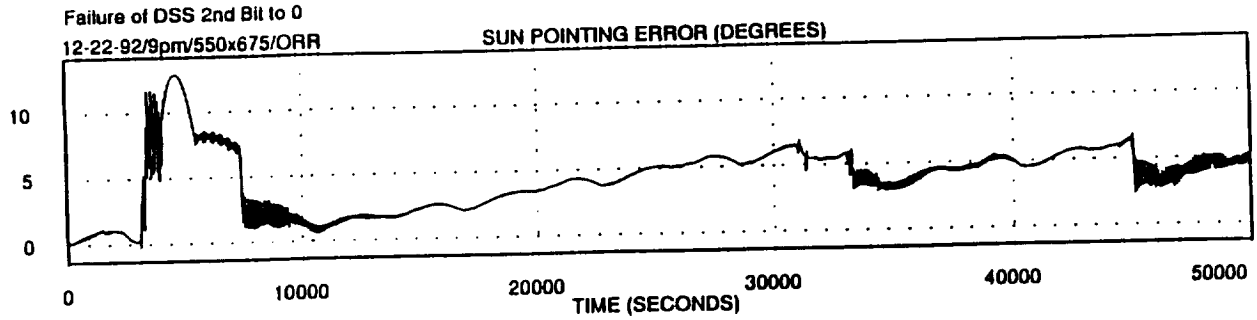

Fig. 10 Sun Pointing Error (Failure of 2nd Bit to 0)

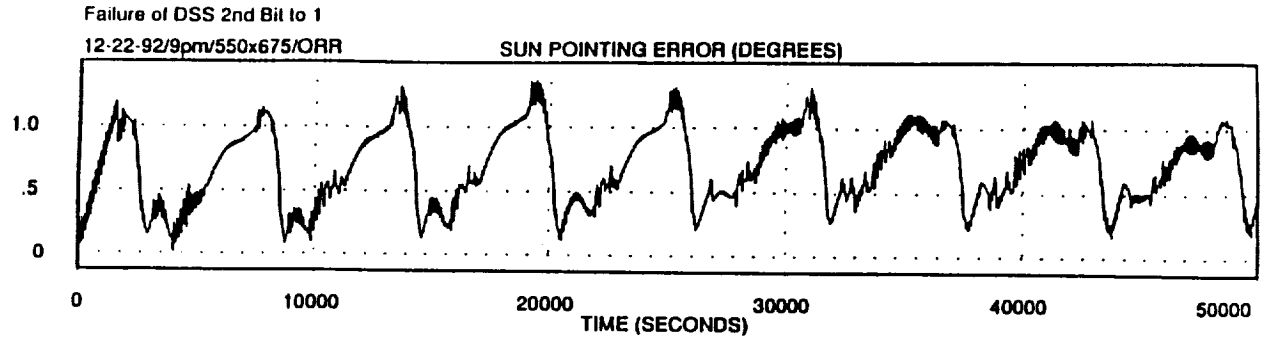

Fig. 11 Sun Pointing Error (Failure of 2nd Bit to 1)

Wheel Failures

Simulations were also run to evaluate the controllability of the spacecraft for a failure in the momentum wheel. The failure was simulated by setting the commanded wheel torque to zero and allowing friction to slow the wheel speed to zero.

The average sun pointing error for a failure in the momentum wheel is approximately 4 degrees in ORR mode. As the wheel speed decreases the momentum of the wheel is distributed to the spacecraft which generates a spin about the pitch axis. Thus, the system momentum vector along the pitch axis is conserved and the magnetic torquers continue to precess this momentum vector towards the sun line. As long as the sun pointing error does not exceed 20 degrees the spacecraft will not enter Safehold.

After initial acquisition, the x and z B-dot controls will be turned off. In this way, if Safehold is entered due to a momentum wheel failure, the spin of the spacecraft will not be damped out, thus conserving the momentum vector needed for sun pointing. It should be noted that the y B-dot control must always be active while in Safehold. The precession control is inherently unstable if it is used by itself. If the sun line is inside the nutation cone, the torques produced by the magnetic torquers will increase any nutation that is present. Therefore, the y B-dot is needed to dampen this nutation.

Magnetometer Failures

The SAMPEX three-axis magnetometer contains an x-axis redundant coil which is available to ORR mode but not to Safehold. If the spacecraft were to enter Safehold with a failure in the primary x-axis coil and sun pointing were not satisfactory, then autonomous switching between the x-axis coils in ORR would be required. Simulations showed an average sun pointing error of 6 degrees in Safehold and the spacecraft remains power safe. Thus, autonomous switching is unnecessary.

Conclusions

The SAMPEX attiude control system has been shown by simulations to meet the SAMPEX mission requirements for sun-pointing and instrument pointing. The velocity avoidance algorithm with a minimum ram angle of 90 degrees added to the orbit rate rotation mode provides the HILT sensor with an 89 percent chance of survival over a three year period without seriously degrading science pointing performance. Larger ram angles cause the spacecraft to flip and seriously decrease science pointing performance. During safehold

mode or when the HILT is switched off for an extended period of time, a retractable cover will be closed to protect the HILT sensor.

Several contingeny cases were analyzed by simulation, to verify that the attitude control algorithms are robust in the presence of sensor or actuator failures. Autonomous logic was added to switch from digital to coarse sun sensor data in the presence of digital sun sensor failures. Simulations of failure of the most significant bit and second significant bit of the digital sun sensor output showed that the failures were either benign or were successfully detected. Adequate sun-pointing performance was maintained for all sun sensor failures studied. Simulations of a momentum wheel failure indicate that the default x and z B-dot switches in Safehold mode be set to open after the initial acquisition phase of the mission Then, if the spacecraft enters Safehold due to a failure in the momentum wheel, the spin of the spacecraft about the pitch axis will not be damped out, and the angular momentum bias produced by the spinning spacecraft will enable SAMPEX to remain sun-pointing. The x and z B-dot switches should be closed during initial acquisition to accomplish acquisition as quickly as possible. Simulations of a failure in the primary x-axis magnetometer show that the sun pointing error remains less than approximately 6 degrees. Thus the spacecraft is in a power safe attitude, and autonomous swithing to the redundant x-axis magnetometer is not required.

The SAMPEX attitude control system algorithms provide robust spacecraft control, and are expected to contribute to a succesful mission.

Acknowledgements

The authors would like to thank Phillip Anz-Meador of Lockheed and Donald Kessler of NASA/JSC. Both were very helpful in providing background information on the orbital debris and micrometeoroid models that they developed. Professor Robert Culp of the University of Colorado also gave useful information on orbital debris. Michael Lauriente and John Ruby, both of NASA/GSFC, provided information on EnviroNET capabilities. Professor Glenn Mason of the University of Maryland, principal investigator of the SMEX/SAMPEX mission, advised the Guidance and Control Branch on the susceptibility of the HILT sensor to hazardous debris. Their contributions were extremely valuable in completing this study.

References

1. Forden, J. K., T. W. Flatley, D. A. Henretty, E. G. Lightsey, and F. L. Markley *On-board Attitude Determination and Control Algorithms for SAMPEX*, NASA/GSFC Flight Mechanics/Estimation Theory Symposium, Greenbelt, MD, May 22-24, 1990.

2. Lerner, Gerald M., *Three-Axis Attitude Determination*, in Spacecraft Attitude Determination and Control, James R. Wertz, editor, D. Reidel, Dordrecht, Holland, 1978.

3. Kessler, D. J., R. C Reynolds, and P. D. Anz-Meador, *Orbital Debris Environment for Spacecraft Designed to Operate in Low Earth Orbit*, NASA Technical Memorandum 100 471, April 1989.

4. Culp, R. D., *Orbital Debris*, 14th Annual AAS Guidance and Control Conference, February 2-6, 1991, Keystone, Colorado.

5. Lauriente, M., NASA/GSFC EnviroNET User Guide, Third Edition, April 2, 1990.

6. Klecker, B., *Study of the Micrometeoroid Hazard for the Experiment HILT/SAMPEX*, Max-Plank-Institut fur Extraterrestrische Physik, December 1990.

7. Grun, E., H. A. Zook, H. Fechtig, and R. H. Giese, *Collisional Balance of the Meteoritic Complex*, Icarus 62 (1985), pp. 244-272.

8. Frakes, J. P., T. W. Flatley, J. K. San, D. A. Henretty, F. L. Markley, and E. G. Lightsey, *SAMPEX Science Pointing with Velocity Avoidance*, AAS Papaer 92-182, AAS/AIAA Spaceflight Mechanics Meeting, Colorado Springs, CO, February 24-26, 1992

9. Lerner, Gerald M., *Sun Sensors*, in Spacecraft Attitude Determination and Control, James R. Wertz, editor, D. Reidel, Dordrecht, Holland, 1978, (Figure 6-15).